Spectroscopic and Electrochemical Evidence for Significant Electronic Coupling in Mixed-Valence Hydrogen-Bonded Adducts of Ruthenium Cyano and Ethylenediamine Complexes

Jie Yang, Dhehinie Seneviratne, Gene Arbatin, Ann Margret Andersson, and Jeff C. Curtis*

Contribution from the Department of Chemistry, University of San Francisco, San Francisco, California

Received July 12, 1996. Revised Manuscript Received December 29, 1996[⊗]

Abstract: Spectroscopic and electrochemical investigations have been carried out on a collection of hydrogen-bonded mixed-valence adducts of ruthenium complexes. The electron donors (H-bond acceptors) are Ru(II) cyano species and the electron acceptors (H-bond donors) are Ru(III) ethylenediamine species, and NIR spectroscopic transitions in the adducts are assigned to intervalence transfer through the hydrogen bonds holding the adducts together (HBIT). Spectroscopic studies using Job's method indicate that the adducts are 2:1 ternary aggregates of formulations such as $[((trpy)(bpy)Ru^{II}(CN))_2,(en)_2Ru^{III}(bpy)]^{5+}$ and $[((bpy)_2Ru^{II}(CN)_2)_2,(en)_2Ru^{III}(bpy)]^{3+}$. Voltammetric investigations show substantial repulsion of the redox waves of the parent complexes in mixtures containing both donor and acceptor. Comparison with known electronic coupling data for mixed-valence ruthenium dimers covalently bound through dithiaspiroalkane bridging ligands indicates that the electronic coupling through H bonds of this type is 65−75% as strong as through σ-covalent bonds.

Introduction

Investigations into the nature and extent of electronic coupling between electron donor and acceptor sites have been a focus of intense activity over a period of many years now. Early approaches pioneered by Hush,[1] Mulliken,[2] and McConnell,[3] among others, have been refined and extended to cover a broad range of experimental systems and to incorporate recent advances in molecular quantum theory.[4−6] One of the most striking areas of recent success has been the convergence of experimental and theoretical work leading to the elucidation of the operative electron tunneling pathways through biopolymers and electron transfer proteins.[7]

Experimentally assessing the degree of electronic wave function decay occurring along each segment of some definable pathway between donor and acceptor remains as one of the outstanding challenges in the field. Beratan and Onuchic have established a successful set of guidelines regarding the various attenuation factors operative across the representative σ-bonded, hydrogen-bonded, and through-space segments of the tunneling pathways relevant to protein environments.[7] Additionally, the importance of the details of structure and bonding along purely σ-bonded pathways to the magnitude of electronic coupling has been established by Curtiss and Miller.[8]

It would be helpful to find systems for which it is possible to experimentally probe electron transfer through pathways involving well-defined H bonds so as to allow for a direct assessment of the attenuation factor relevant to the H-bonded link, or at least so as to compare the efficiency of electron transfer relative to covalently bonded pathways in related systems. Relevant to this point, systems have now been designed and investigated in which both energy[9] and electron[10 −12] transfer is unambiguously shown to occur through H bonds. Especially informative are the thermal rate measurements of Therien and co-workers across dicarboxylate H-bonded bridges between metalloporphyrin systems which show that electron transfer can be surprisingly facile through at least this kind of H-bonded pathway;[11] their analysis suggests that the coupling through the H bonds is as good as, or perhaps even stronger than, that through structurally analogous covalent σ bonds.

We report here on work with a set of inorganic complexes relevant to the goal of comparing electronic coupling through H bonds with coupling through covalent bonds. Our studies

[⊗] Abstract published in *Advance ACS Abstracts,* May 15, 1997.

(1) (a) Hush, N. S. *J. Chem. Phys.* **1958**, *28*, 962. (b) Hush, N. S. *Trans. Faraday Soc.* **1961**, *57*, 557. (c) Hush, N. S. *Prog. Inorg. Chem.* **1967**, *8*, 391.

(2) Mulliken, R. S.; Person, W. B. *Molecular Complexes*; Wiley: New York, 1969.

(3) McConnell, H. M. *J. Chem. Phys.* **1961**, *35*, 508.

(4) (a) Reimers, J. R.; Hush, N. S. *Chem. Phys.* **1989**, *134*, 323. (b) Reimers, J. R.; Hush, N. S. *Adv. Chem. Ser.* **1990**, *226*, 27.

(5) (a) Cave, R. J.; Newton, M. D. *Chem. Phys. Lett.* **1996**, *249*, 15. (b) Liu, Y. P.; Newton, M. D. *J. Phys. Chem.* **1995**, *99*, 12382. (c) Cave, R. J.; Newton, M. D.; Kumar, K.; Zimmt, M. B. *J. Phys. Chem.* **1995**, *99*, 17501. (d) Newton, M. D. *Chem. Rev.* **1991**, *91*, 767.

(6) (a) Hupp, J. T. *J. Am. Chem. Soc.* **1990**, *112*, 1563−1565. (b) Richardson, D. E.; Taube, H. *J. Am. Chem. Soc.* **1983**, *105*, 40. (c) Piepho, S. B. *J. Am. Chem. Soc.* **1990**, *112*, 4197. (d) Piepho, S. B., *J. Am. Chem. Soc.* **1988**, *110*, 6319. (e) Wong, K. Y.; Schatz, P. N.; Piepho, S. B., *J. Am. Chem. Soc.* **1979**, *101*, 2793. (f) Zhang, L. T.; Ko, J.; Ondrechen, M. J., *J. Am. Chem. Soc.* **1987**, *109*, 1666. (g) Zhang, L. T.; Ko, J.; Ondrechen, M. J. *J. Phys. Chem.* **1989**, *93*, 3030. (h) Todd, M. D.; Nitzan, A.; Ratner, M. A. *J. Phys. Chem.* **1993**, *97*, 29. (i) Mikkelsen, K. V.; Ratner, M. A. *J. Am. Chem. Soc.* **1989**, *93*, 1759.

(7) (a) Beratan, D. N.; Onuchic, J. N. *Adv. Chem. Ser.* **1991**, *228*, 71. (b) Therien, M. J.; Bowler, B. E.; Selman, M. A.; Gray, H. B.; Chang, I. J.; Winkler, J. R. *Adv. Chem. Ser.* **1991**, 228. (c) Beratan, D. N.; Onuchic, J. N.; Winkler, J. R.; Gray, H. B. *Science* **1992**, *258*, 1740. (d) Beratan, D. N.; Betts, J. N.; Onuchic, J. N. *J. Phys. Chem.* **1992**, *96*, 2852. (e) Regan, J. J.; Bilio, A. D.; Langen, R.; Skov, L. K.; Winkler, J. R.; Gray, H. B.; Onuchic, J. N. *Chem. Biol.* **1995**, *2*, 489.

(8) (a) Curtiss, L. A.; Naleway, C. A.; Miller, J. R. *J. Phys. Chem.* **1995**, *99*, 1182. (b) Paulson, B. P.; Curtiss, L. A.; Bal, B.; Closs, G. L.; Miller, J. R. *J. Am. Chem. Soc.* **1996**, *118*, 378.

(9) (a) Harriman, A.; Magda, D. J.; Sessler, J. L. *J. Phys.Chem.* **1991**, *95*, 1530−1532. (b) Sessler, J. L.; Wang, B.; Harriman, A. *J. Am. Chem. Soc.* **1995**, *117*, 704−714. (c) Kral, V.; Springs, S. L.; Sessler, J. L. *J. Am. Chem. Soc.* **1995**, *117*, 8881−8882.

(10) (a) Harriman, A.; Kubo, Y.; Sessler, J. L. *J. Am. Chem. Soc.* **1992**, *114*, 388−390. (b) Sessler, J. L.; Wang, B.; Harriman, A. *J. Am. Chem. Soc.* **1993**, *115*, 10418−10419.

(11) de Rege, P. J. F.; Williams, S. A.; Therein, M. J. *Science* **1995**, *269*, 1409.

(12) (a) Roberts, J. A.; Kirby, J. P.; Nocera, D. G. *J. Am. Chem. Soc.* **1995**, *117*, 8051. (b) Cukier, R. I. *J. Phys. Chem.* **1995**, *99*, 16101.

S0002-7863(96)02391-8 CCC: $14.00

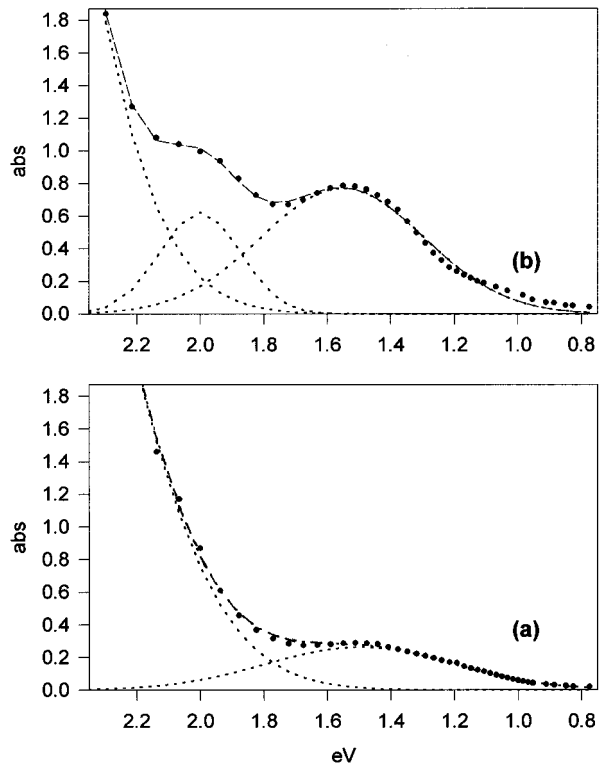

Figure 1. HBIT specta and spectral deconvolutions for (a) $[((trpy)(bpy)Ru^{II}(CN))_2,(en)_2Ru^{III}(bpy)]^{5+}$ and (b)$[((bpy)_2Ru^{II}(CN)_2)_2,(en)_2Ru^{III}(bpy)]^{3+}$ in acetonitrile (5 cm path length).

center around two lines of experimental evidence which indicate significant electronic coupling across hydrogen bonds in mixed-valence hydrogen-bonded adducts formed between ruthenium(II) electron-donor and ruthenium(III) electron-acceptor complexes in solution. We find that in acetonitrile or nitromethane as solvent, H-bonded adducts between cyano-bearing Ru(II) and ethylenediamine-bearing Ru(III) species such as the ones shown in eq 1 below will form with high association constant. These adducts exhibit weak intervalence-transfer transitions in the low energy visible and near infrared regions which are not present in either reduced or oxidized solutions of either complex alone and which cannot be ascribed to a simple halide ion-to-metal charge transfer originating from the bromide ion formed upon oxidation of the $(en)_2Ru^{II}(bpy)^{2+}$ species.[13,14]

$$2(trpy)(bpy)Ru^{II}(CN)^{+} + (en)_2Ru^{II}(bpy)^{2+} \xrightarrow{Br_2} [((trpy)(bpy)Ru^{II}(CN))_2,(en)_2Ru^{III}(bpy)]^{5+} + Br^{-} \quad (1)$$

1

The spectroscopic transition corresponds to the optical electron-transfer process shown in eq 2 below, and two examples of H-bonded intervalence-transfer (HBIT) spectra are shown in Figure 1.

$$[((trpy)(bpy)Ru^{II}(CN)\cdots HN-Ru^{III}(bpy)),(CN)Ru^{II}(bpy)(tpy)]^{5+} \xrightarrow{h\nu} [((trpy)(bpy)Ru^{III}(CN)\cdots HN-Ru^{II}(bpy)),(CN)Ru^{II}(bpy)(tpy)]^{5+*} \quad (2)$$

where $Ru^{II}(CN)\cdots HN-Ru^{III}$ is meant here to depict a hydrogen-bonding interaction between the cyano ligand on the Ru(II) complex and one of the N-bound amine hydrogens of ethylenediamine on the Ru(III) complex (the basicity of cyano ligands on Ru(II) is well-established[15] as is the Lewis acidity of the amine hydrogens in metal−en complexes[16,17]).

The interaction between the redox sites in the H-bonded adducts is also evident in the redox potentials of mixtures of the two species together relative to the potentials observed in pure solutions of either species alone; the redox waves for the isolated parent complexes are found to repell each other in mixtures of the two in low-donor number[17] solvents. As will be discussed, the solvent dependence of this electrochemical interaction supports the presumed role of H bonds in driving the adduct formation.

Experimental Section

The ruthenium trichloride starting material used in this study was obtained from Alpha-Aesar under the Platinum Group Metals loan program. The ligands employed, ethylenediamine (en), 2,2′-bipyridine (bpy), 4,4′-dimethyl-2,2′-bipyridine (dmbpy), 3,4,7,8-tetramethyl-1,10-phenanthroline (tmphen), and 2,2′,2″-terpyridine (trpy) were purchased from Aldrich and used without further purification. The solvents used, nitromethane (NM), acetonitrile (AN), acetone (AC), dimethylformamide (DMF), and dimethyl sulfoxide (DMSO), were obtained as spectro- or HPLC-grade from either Aldrich or VWR and were dried by passing them over a column of activated, weakly acidic alumina (VWR) prior to use.

$Ru(bpy)_2Cl_2$ and $Ru(dmbpy)_2Cl_2$. These starting materials were synthesized according to the method reported by Sullivan *et al.*[18] Before use in the next step, the crude products were purified once by suspending them in hot 0.1 M NaCl in water and then precipitating the dark green-black product by refrigeration at 0 °C. The purified product was then isolated by filtration and dried under vacuum.

$Ru(bpy)_2(CN)_2$ and $Ru(dmbpy)_2(CN)_2$. These compounds were also synthesized according to ref 18, but with minor modifications. In a typical preparation, 0.25 g of $Ru(bpy)_2Cl_2$ or $Ru(dmbpy)_2Cl_2$ was heated at relux for 5 h in 50% ethanol−water with 5 equiv of KCN. After cooling, the ethanol was removed by rotary evaporation and the crude product that precipitated from the water was isolated by filtration. Yields were typically 70%. The crude material was purified similarly to chloride described above (substituting 0.05 M KCN for 0.1 M NaCl). Microanalytical data are given in Table 1, and UV−vis/electroanalytical data are given in Table 2.

$Ru(trpy)(Cl)_3$. This starting material was synthesized according to the method of Sullivan *et* al.[19] of $RuCl_3(H_2O)_x$ (0.262 g) and 233 mg of 2,2′,2″-terpyridine in 125 mL of absolute ethanol were heated at reflux for 3 h. Thereafter, the mixture was cooled to room tempareture and the fine brownish-yellow product was isolated by filtration, washed with three 30-mL portions of 50:50 absolute ethanol−diethyl ether, and then air dried. Typical yields were 80%.

$Ru(trpy)(bpy)Cl(PF_6)$. $Ru(trpy)(Cl)_3$ (0.33 g) was added to 70 mL of 7:3 ethanol−water, and the mixture was heated at reflux for 2 h in the presence of 0.35 g (3 equiv) of 2,2′-bpy. The mixture was then cooled to room temperature and the ethanol was removed by rotary evaporation. Three equivalents of NH_4PF_6 (0.35 g) were added to the aqueous solution of the product, and the mixture was chilled at 0 °C. The product was isolated by filtration and dried in vacuum. Subsequent to this, the crude product was reprecipitated from acetone solution *via* addition of excess diethyl ether (usually required 4−5 volumes).

(13) Sexton, D. A.; Curtis, J. C.; Cohen, H.; Ford, P. C. *Inorg. Chem.* **1984**, *23*, 49.

(14) trpy is 2,2′,2″-terpyridine, bpy is 2,2′-bipyridine, and en is ethylenediamine.

(15) (a) Demas, J. N.; Addington, J. W. *J. Am. Chem. Soc.* **1974**, *96*, 3663. (b) Peterson, S. H.; Demas, J. N. *J. Am. Chem. Soc.* **1976**, *98*, 7880. (c) Peterson, S. H.; Demas, J. N. *J. Am. Chem. Soc.* **1979**, *101*, 6571. (d) Demas, J. N.; Addington, J. W.; Peterson, S. H.; Harris, E. W. *J. Phys. Chem.* **1977**, *81*, 1039.

(16) (a) Mayer, U.; Kotocova, A.; Gutmann, V.; Gerger, W. *J. Electroanal. Chem.* **1979**, *100*, 875. (b) Farmer, P. J.; Cave, J. R.; Fletcher, J. A.; Rhubottom, J. A.; Walmsley, J. A. *Inorg. Chem.* **1991**, *30*, 3414−3420.

(17) (a) Gutmann, V. *The Donor−Acceptor Approach to Molecular Interactions*; Plenum: New York, 1978. (b) Marcus, Y. *J. Solution Chem.* **1984**, *13*, 599.

(18) Sullivan, B. P.; Salmon, D. J.; Meyer, T. J. *Inorg. Chem.* **1978**, *17*, 3334.

(19) Sullivan, B. P.; Calvert, J. M.; Meyer, T. J. *Inorg. Chem.* **1980**, *19*, 1404.

Table 1. Microanalytical Data for the Various Complexes Used in This Study

formula	% C theory (obsd)	% H theory (obsd)	% N theory (obsd)
$Ru(bpy)_2(CN)_2 \cdot 2H_2O$	52.68 (52.85)	4.02 (4.27)	16.76 (16.83)
$Ru(dmbpy)_2(CN)_2 \cdot 3H_2O$	54.24 (53.94)	5.25 (5.31)	14.60 (14.64)
$Ru(trpy)(bpy)CN(PF_6) \cdot H_2O$	45.95 (46.22)	3.11 (3.58)	12.37 (12.53)
$Ru(en)_2(bpy)(PF_6)_2$	25.19 (24.45)	3.62 (3.70)	12.59 (12.62)
$Ru(en)_2(dmbpy)(PF_6)_2 \cdot$(acetone)	30.28 (29.87)	4.55 (4.59)	11.15 (11.03)
$Ru(en)_2(tmphen)(PF_6)_2 \cdot H_2O$	31.21 (31.64)	4.97 (4.63)	10.92 (10.83)

Table 2. UV-Vis and Electroanalytical Characterization Data for the Complexes Used in This Study

	acetonitrile		nitromethane	
solvent	λ_{max}, nm (ϵ_{max})	$E_{1/2}$,[a] V	λ_{max} nm (ϵ_{max})	$E_{1/2}$,[a] V
$Ru(bpy)_2(CN)_2$	244 (22050)	0.444		0.480
	293 (58820)			
	342 (8820)			
	493 (10000)		490 (7600)	
$Ru(dmbpy)_2(CN)_2$	234 (42400)	0.347		0.362
	256 (23800)			
	282 (53000)		376 (7000)	
	424 (8200)		486 (9920)	
$Ru(trpy)(bpy)CN(PF_6)$	290 (38000)	0.665		0.685
	312 (34000)			
	470 (9050)		484 (10120)	
$Ru(bpy)(en)_2(PF_6)_2$	296 (39000)	0.226		0.371
	366 (9500)		376 (7000)	
	518 (6200)		508 (6300)	
$Ru(dmbpy)(en)_2(PF_6)_2$	250 (9600)	0.176		0.301
	294 (25000)			
	366 (6300)		378 (5700)	
	518 (4000)		504 (4600)	
$Ru(tmphen)(en)_2(PF_6)_2$	234 (18000)	0.143		0.263
	274 (33400)			
	464 (5200)		454 (8000)	

[a] $E_{1/2}$ measured *vs* fc/fc^+ reference couple.

Typical yields were 75%. The compound was further purified by column chromatography on weakly acidic alumina using 3:1 toluene−acetonitrile as eluent with up to 1% added methanol toward the end. The desired product was the first band. The fraction of eluent containing this band was collected and the purified product was precipitated by removing the acetonitrile fraction of the eluent on a rotary evaporator. The resulting solid was isolated by filtration and then reprecipitated once from acetone−diethyl ether as described above.

$Ru(trpy)(bpy)CN(PF_6)$. Ru(trpy)(bpy)Cl(PF6) (0.26 g) was heated at reflux in 20 mL of 7:3 ethanol−water for 3 h in the presence of 0.09 g (3 equiv) of KCN. Upon cooling, 0.1 g of NH_4PF_6 was added and the ethanol was removed by rotary evaporation.

The crude orange-red solid was isolated by filtration, dried in vacuum, and then reprecipitated from acetone via addition of excess diethyl ether. The compound was further purified by column chromatography on weakly acidic alumina with 3:1 toluene−acetonitrile as eluent with up to 2% added methanol toward the end. The desired product was the first band. The fraction of eluent containing this band was collected, and the solid was precipitated by removing the solvent on a rotary evaporator. The resulting solid was isolated by filtration and then reprecipitated once from acetone−diethyl ether. Microanalytical data are given in Table 1 and UV−vis/electroanalytical data are given in Table 2.

$Ru(bpy)Cl_4$, $Ru(dmbpy)Cl_4$, and $Ru(tmphen)Cl_4$. These starting materials were synthesized according to the methods described by Dwyer *et al.*[20] and by Krauze[21] and then reacted without isolation to go on to the desired ethylenediamine product.

$Ru(bpy)(en)_2(PF_6)_2$, $Ru(dmbpy)(en)_2(PF_6)_2$, and $Ru(tmphen)(en)_2(PF_6)_2$. In a typical synthesis, 0.25 g of $RuCl_3 \cdot 3H_2O$ was dissolved in 40 mL of 20% ethanol in water in a 100- mL round-bottom flask, and 1 equiv of heterocyclic ligand (bpy, dmbpy, or tmphen) was added slowly over a 1-h period with stirring and gentle warming of the solution (40−50 °C). The solution was then heated at reflux for 4 h with stirring. The solution was then cooled to room temperature, and 10 equiv of ethylenediamine (0.6 mL) was added with stirring (the reaction may be stopped prior to adding ethylenediamine and kept at 0 °C overnight). The solution was then heated at reflux again for 6 h and cooled to room temperature, and 2.5 equiv of NH_4PF_6 (0.4 g) was added with stirring. The ethanol was removed by rotary evaporation, and the crude, dark red precipitate was isolated by filtration and dried in vacuum. Typical crude product yields were 70%. The crude solid was then dried in vacuum and reprecipitated from acetone−diethyl ether. Final purification was accomplished by column chromatography on alumina as described above for the $Ru(trpy)(bpy)CN(PF_6)$ complex. Microanalytical data are given in Table 1, and UV−vis/electroanalytical data are given in Table 2.

Electroanalytical Measurements. Differential pulse, cyclic, and square-wave voltammograms were obtained with an EG&G PARC Versatat computer-controlled electrochemical analyzer. The supporting electrolyte in all cases was tetraethylammonium hexafluorphosphate (TEAH) synthesized according to the method described by Chang et. al.[22] Electrochemical investigations of the H-bonded adducts as a function of solvent were carried out on both platinum and glassy carbon disk electrodes. We obtained the best performance (as judged by peak symmetry and signal-to-noise ratio at a given concentration) in the high donor solvents (DMF, DMSO) using glassy carbon as the electrode material and square-wave voltammetry as the technique (with sweep rates of at least 20 mV/s). Peak postions were independent of electrode material, but the slower technique of differential pulse polarography, especially on platinum, gave rise to asymmetric peaks and in some cases spurious peaks not observed at all on glassy carbon. In the low-donor solvents (NM, AN) the platinum electrode performed best and essentially identical results were obtained with either square-wave voltammetry or differential pulse voltammetry. In the mid-range donicity solvent acetone, AC, results were the same for both electode materials and both techniques.

Spectroscopic Measurements. Routine UV−vis spectra for measurement of extinction coefficients were obtained either on a Perkin-Elmer 330 UV−vis−NIR scanning spectrophotometer or a Hewlett-Packard 8452A diode array intrument. Vis−NIR spectra recorded to study the HBIT band were mostly obtained in 5-cm cells at concentrations in the range of 0.3−0.8 mM in each metal complex (e.g., $Ru(bpy)_2(CN)_2$ and $Ru(en)_2(bpy)(PF_6)_2$). The mixed-valence adduct was generated by in-situ oxidation with small portions of bromine vapor delivered by a pastuer pipet (in a hood well-removed from the spectrophotometer). Care must be taken not to overshoot the maximum absorbance at the wavelength of the HBIT band by adding too much Br_2. Other oxidants such as cericammonium nitrate or $Fe(bpy)_3(PF_6)_3$ could be used to generate the mixed-valence species,[22] but the results were less reproducible, and in the case of the former oxidant precipitation of the oxidized products usually occurred.

In a typical study of the HBIT band, the NIR region from 1600 to about 550 nm was scanned at 0−0.5 au full scale. The scale was switched to 0−4 au full scale toward the short-wavelength extreme so as to map out as much as possible of the intense MLCT region tail of the cyano complex (for purposes of obtaining the best possible spectral deconvolution of the HBIT band). Spectral deconvolution was performed by digitizing the absorbance vs wavelength data, converting to absorbance *vs* energy (eV), and then using the curve-fitting function within Sigmaplot for Windows (Jandel Scientific) to perform the decompostion into a single Gaussian band for the low-energy HBIT

(20) Dwyer, F. P.; Goodwin, H. A.; Gyarfas, E. C. *Aust. J. Chem.* **1962**, *16*, 42−50.

(21) Krause, R. A. *Inorg. Chim. Acta* **1977**, *22*, 209−213.

(22) Chang, P. J.; Fung, E. Y.; Salaymeh, F.; Curtis, J. C. *Inorg. Chem.* **1986**, *25*, 4233−4241.

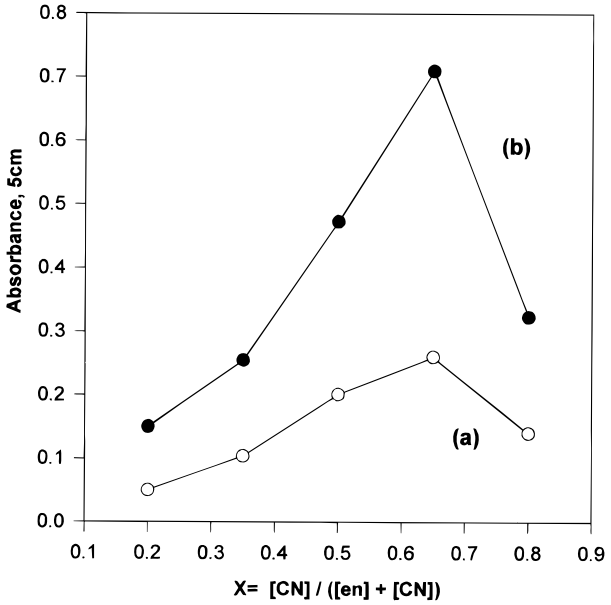

Figure 2. Job's plots for (a) $[((trpy)(bpy)Ru^{II}(CN))_2,(en)_2Ru^{III}(bpy)]^{5+}$ at 925 nm and (b) $[((bpy)_2Ru^{II}(CN)_2)_2,(en)_2Ru^{III}(bpy)]^{3+}$ in nitromethane at 830 nm.

band and the steeply rising peak on the high-energy side as a best fit for the MLCT tail (see Figure 1 for an illustration of the spectral fits). In NM and AN in the cases of adducts formed from dicyano donor complexes, a second somewhat higher energy NIR band could be seen if the the donor species was in sufficient excess over the acceptor species (*vide infra*). In these cases, deconvolution of the lower-energy band required two separate Gaussians as well as the tail on the high-energy side.

Modeling Studies. The molecular mechanics calculations performed on the H-bonded adducts were done with the MM+ program included in the Hyperchem 4.5 suite of programs (Hypercube). The renderings shown in Figures 6 and 7 were made with Hyperchem's Chemplus extension.

Results and Discussion

Figure 1, parts a and b, shows the HBIT spectra and deconvolutions from the higher-lying and more intense MLCT band of the Ru(II) cyano donor species for adduct **1**, $[((trpy)(bpy)Ru^{II}(CN))_2,(en)_2Ru^{III}(bpy)]^{5+}$, which is formed from the monocyano donor complex $(trpy)(bpy)Ru^{II}(CN)^+$, and adduct **2**, $[((bpy)_2Ru^{II}(CN)_2)_2,(en)_2Ru^{III}(bpy)]^{3+}$, which is formed from the dicyano donor complex $(bpy)_2Ru^{II}(CN)_2$. These spectra are recorded at the donor−acceptor mole ratio of 2:1 in accordance with the Job's plot[23] results for the HBIT band shown in Figure 2, parts a and b. The Job's plots clearly maximize at 0.65, indicative of a 2:1 mole ratio for the absorbing species. Thus the extinction coefficients reported with the spectral data summarized in Table 3 are based on the concentration of the Ru(III) electron-accepting species and the absorbance maxima resulting from spectral deconvolution. The 2:1 Ru(II)−Ru(III) ratio implied by the Job's plot requires that we divide the observed extinction coefficient values by two if we wish to consider the intensity of the HBIT transition on a *per metal−metal interaction* basis (*vide infra*).

In some cases the spectral analysis is complicated by the onset of a second HBIT absorption at higher energy, which begins to become significant at Job's fractions ≥0.65 (meaning a ≥2:1 Ru(II)−Ru(III) ratio). The higher energy peak (generally a poorly-resolved shoulder on the MLCT tail) is most apparent for adducts of dicyano donor complexes in the low-donicity solvent nitromethane, and we attribute the new peak to the probable formation of higher order, e.g., 3:1 mole ratio, aggregates.[24] The existence of at least some small amount of higher-order aggregate even at the 2:1 mixing ratio for some of the complexes requires that the extinction coefficient reported for these cases in Table 3 must be corrected to reflect the area fraction of total IT absorption due specifically to the low-energy, main component. These area fractions (obtained via deconvolution) are noted in the table. The Job's plots experiments show that the higher-energy peak grows at the expense of the lower-energy one for mole fractions of dicyano complex corresponding to ratios greater than 2:1.

Beer's law plots for HBIT bands of adducts **1** and **2** are shown in Figure 3. The plots are linear within error all the way down to our practical detection limit of 0.4 mM in 5 cm cells. If we assume a minimum of 90% adduct formation at the low end, we are able to calculate a least lower bound of $K_f \geq 3000\ M^{-1}$

Table 3. HBIT Spectral Data[a] for Various Pairs of Ru^{II} Cyano/Ru^{III} Ethylenediamine Complexes as H-Bonded Adducts at 2:1 Donor−Acceptor Molar Ratio

adduct	solvent	l_{max}, nm	n_{max}, eV	$Dn_{1/2}$, eV	e_{max},[b] $M^{-1}\,cm^{-1}$	H_{ab},[f] eV
$[(Ru(trpy)(bpy)(CN))_2,(Ru(bpy)(en)_2)]^{4+}$	AN	886	1.40	0.67	290[c]	0.034
$[(Ru(trpy)(bpy)(CN))_2,(Ru(bpy)(en)_2)]^{4+}$	NM	925	1.34	0.84	95[c]	0.021
$[(Ru(trpy)(bpy)(CN))_2,(Ru(tmphen)(en)_2)]^{4+}$	AN	954	1.30	0.61	250[d]	0.029
$[(Ru(bpy)_2(CN)_2)_2,(Ru(bpy)(en)_2)]^{3+}$	NM	826	1.50	0.46	1570[d] (0.43[e])	0.078[g]
$[(Ru(bpy)_2(CN)_2)_2,(Ru(bpy)(en)_2)]^{3+}$	AN	775	1.60	0.71	1050[c] (0.75[e])	0.081[g]
$[(Ru(dmbpy)_2(CN)_2)_2,(Ru(bpy)(en)_2)]^{3+}$	NM	785	1.58	0.68	450[c] (0.60[e])	0.052[g]
$[(Ru(dmbpy)_2(CN)_2)_2,(Ru(bpy)(en)_2)]^{3+}$	AN	795	1.56	0.59	670[d] (0.58[e])	0.058[g]
$[(Ru(dmbpy)_2(CN)_2)_2,(Ru(dmbpy)(en)_2)]^{3+}$	NM	827	1.50	0.96	640[d] (0.65[e])	0.072[g]
$[(Ru(dmbpy)_2(CN)_2)_2,(Ru(tmphen)(en)_2)]^{3+}$	NM	838	1.48	0.59	930[d] (0.34[e])	0.067[g]

[a] HBIT band parameters obtained via spectral deconvolution as described in text and illustrated in Figure 1. [b] ϵ_{max} is calculated here on the basis of the $Ru^{III}(en)_2(LL)^{3+}$ acceptor complex concentration. [c] ϵ_{max} calculated from the slope of the absorbance vs concentration linearity plot. [d] ϵ_{max} obtained from a single point determination. [e] In the adducts of the dicyano complexes at a Job's mole fraction of Ru^{II} ≥ 0.65 a higher-energy I. T. band due to higher aggregate formation starts to become significant (see Figure 1b). The number in parentheses is the area fraction of total I. T. absorption due to the low-energy component, and this fraction is used in calculation of ϵ_{max}. [f] H_{ab} calculated here on a *per metal−metal interaction* basis (the ϵ_{max} value used in eq 4 is thus one half of the ϵ_{max} value reported in this table in order to account for the existence of *two* metal−metal interactions per adduct). The distance used is in the middle of the estimated range for each adduct; 7.1 Å for the (trpy)(bpy)(CN) adducts and 6.2 Å for the $(bpy)_2(CN)_2$ adducts (see text). [g] These H_{ab} values are calculated on a per metal−metal interaction basis assuming two metal−metal interactions per 2:1 adduct. Assuming two H bonds per metal−metal interaction would lead to values half this large on a per H-bond basis; see text and Figure 8; point **b** is on a per H-bond basis assuming two H bonds per metal−metal interaction.

(23) In the Job's plot method one varies the molar ratio of two species in solution while keeping the total moles constant so as to identify the stoichiometry of any complex or adduct formed. See, for example: Harris, D. *Quantitative Methods of Chemical Analysis*, 2nd ed.; W. H. Freeman and Co.: New York, 1987; pp 519−521. The adducts we investigated in this manner, $(bpy)_2Ru^{II}(CN)_2$ and $(en)_2Ru^{III}(bpy)^{3+}$ in both NM and AN, $(trpy)(bpy)Ru^{II}(CN)^+$ and $(en)_2Ru^{III}(bpy)^{3+}$ in both NM and AN, and $(dmbpy)_2Ru^{II}(CN)_2$ and $(en)_2Ru^{III}(dmbpy)^{3+}$ in NM, all displayed clear peaks at a Job's parameter of 0.65 with respect to cyano complex, indicating that the absorbing species in solution were all of the composition ratio $[(Ru^{II}\text{-cyano})_2,((en)_2Ru^{III})]^{n+}$.

(24) Spectroscopic and kinetic evidence of multiple cyano complexes binding to a central ammine complex have been demonstrated recently by Taube and co-workers; Poulopoulou, V. G.; Taube, H. In press.

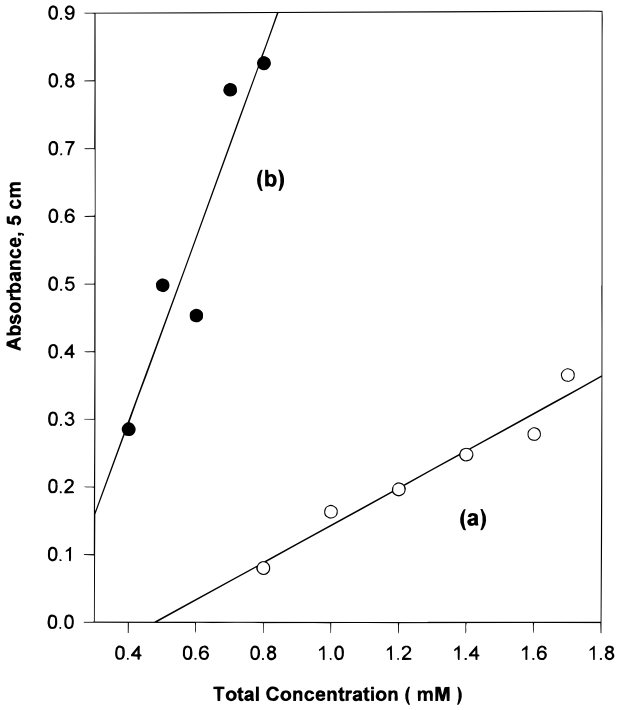

Figure 3. Beer's law plots for (a) $[((trpy)(bpy)Ru^{II}(CN))_2,(en)_2Ru^{III}(bpy)]^{5+}$ in nitromethane at 920 nm and (b) $[((bpy)_2Ru^{II}(CN)_2)_2,(en)_2Ru^{III}(bpy)]^{3+}$ in acetonitrile at 800 nm.

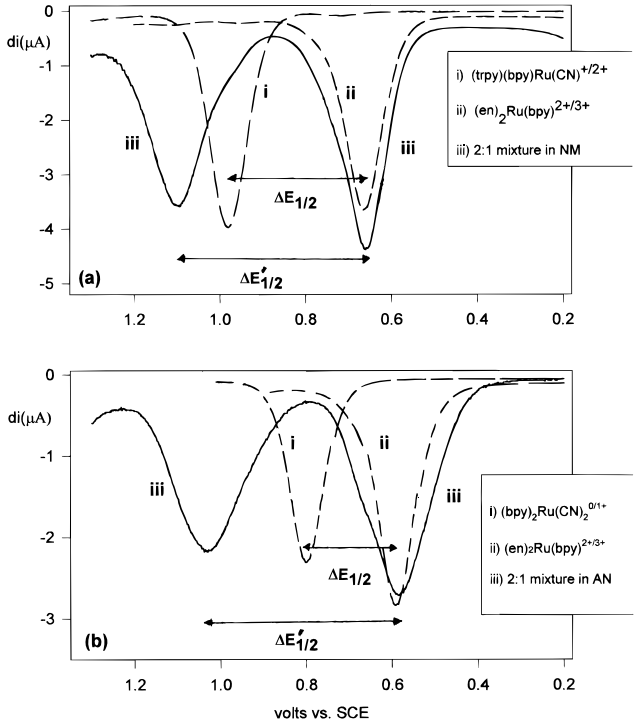

Figure 4. Differential pulse voltammograms illustrating the wave repulsion effect for adducts **1** and **2** in both NM and AN solvents. E_{rep} identical with $\Delta E_{1/2}' - \Delta E_{1/2}$.

for the equilibrium constant for adduct formation. The electrochemical data are in qualitative agreement with this conclusion since the H-bonded interaction as evidenced by the electrochemical wave-repulsion effect *(vide infra*) is fully developed even at the lowest limit of our confident detection ability (~0.08 mM).

Figure 4 shows how the differential pulse polarograpic waves for the isolated cyano- and ethylenediamine complexes repel in their mixtures in low-to-moderate donor strength solvents where adduct formation according to eq 1 is complete. As is the case with the NIR studies of the HBIT band, the dicyano-based adducts display somewhat more complex behavior than the monocyano ones; Figure 4b shows that the peaks can become significantly asymmetric and show signs of beginning to split into multiple peaks. Although we have no detailed scheme to account for this structure, we note that it is broadly consistent with the idea of higher aggregate formation for the dicyano species[24,25] since adducts with varying structures and/or composition ratios might be expected to display slightly different free energies of oxidation and reduction. Most of the wave repulsion effect shows up as an anodic shift in the half-wave potential of the cyano complex. This is different from what is generally seen with dimeric, covalently-bridged ruthenium complexes where the potentials of both ends of the dimer are shifted significantly relative the appropriate monomeric species.[26]

The electrochemical data for adducts **1** and **2** as a function of solvent are summarized in Table 4 and displayed in Figure 5. We see that the wave repulsion effect falls away to zero as we go from low-donicity solvents such as nitromethane and nitrobenzene to the high-donicity solvents DMSO and DMF. This behavior supports the idea that H bonding between the donor and acceptor is the predominant factor in holding the adducts together; it is unlikely that ring-stacking interactions or charge resonance-derived forces would display this solvent dependence. The simplest interpretation is that the high donor number solvents (stronger Lewis bases) such as DMSO and DMF compete effectively with the cyano complexes for the Lewis-acidic, N-bound ethylenediamine protons of the Ru(III) acceptor complex and thus inhibit adduct formation.

The voltammetric wave repulsion that arises between the electronically interacting redox sites will contribute to the favorable free energy of comproportionation, ΔG_{com}, depicted in (3) below,

$$2[((trpy)(bpy)Ru^{II}(CN))_2,(en)_2Ru^{II}(bpy)]^{4+} + [((trpy)(bpy)Ru^{III}(CN))_2,(en)_2Ru^{III}(bpy)]^{7+} \rightarrow 3[((trpy)(bpy)Ru^{II}(CN))_2,(en)_2Ru^{III}(bpy)]^{5+} \quad (3)$$

$$\Delta G_{com} = -nF(\Delta E_{1/2}')$$

where $\Delta E_{1/2}'$ is the total observed voltammetric wave splitting in volts (see Figure 4) and $n = 2$. The magnitude of E_{rep} (defined as $E_{rep} \equiv \Delta E_{1/2}' - \Delta E_{1/2}$, see Figure 4), which arises in the mixed-valence H-bonded adducts of the parent complexes, varies with the number of cyano groups on the Ru(II) donor complex. Monocyano adduct **1** shown above in nitromethane as solvent, for example, exhibits a total wave splitting $\Delta E_{1/2}'$ of 0.447 V and a wave repulsion E_{rep} of 0.131 V relative to the isolated parent complexes. This allows us to calculate that $\Delta G_{com} = 86.3$ kJ/mol, with 25.2 kJ/mol of this arising somehow from the donor−acceptor interaction. For dicyano adduct **2** in

(25) MM+ molecular mechanics modeling studies indicate that 3:1 adducts involving 3 dicyano elecrtron-donor species bound to a single $(en)_2Ru^{III}$ ion, of the formulation $[((bpy)_2Ru^{II}(CN)_2)_3,(en)_2Ru^{III}(bpy)]^{3+}$, are less sterically crowded than 3:1 adducts formed from the monocyano donor $(trpy)(bpy)Ru^{II}(CN)^+$ due to the steric requirements of the fifth hetercyclic ring in the monocyano complexes, thus experimental evidence for facile formation of higher aggregates of the dicyano donors but not the monocyano ones is at least rationalizable at this level of theory. Electrostatic considerations would also point in this direction.

(26) (a) Salaymeh, F. S.; Berhane, S.; Yusof, R.; de la Rosa, R.; Fung, E. Y.; Matamoros, R.; Lau, K.; Qian, Z.; Kober, E.; Curtis, J. C. *Inorg. Chem.* **1993**, *32*, 3895−3908. (b) Narvor, N. L.; Toupet, L.; Lapinte, C. *J. Am. Chem. Soc.* **1995**, *117*, 7129−7138.

Table 4. Electrochemical Data Summarizing the Behavior of E_{rep} as a Function of Solvent Donor Number for Solutions of 2:1 Mixtures of Parent Complexes Leading to Mixed-Valence Adducts **1** and **2**[a]

		$[((bpy)_2Ru^{II}(CN)_2)_2, (en)_2Ru^{III}(bpy)]^{3+}$			$[((trpy)(bpy)Ru^{II}(CN))_2, (en)_2Ru^{III}(bpy)]^{5+}$		
solvent	donor no.	$E_{1/2}(1)$	$E_{1/2}(2)$	E_{rep}	$E_{1/2}(1)$	$E_{1/2}(2)$	E_{rep}
nitromethane (NM)	2.7	0.247	0.616	0.262	0.359	0.806	0.131
nitrobenzene (NB)	4.4	0.257	0.717	0.358	0.302	0.839	0.185
benzonitrile (BN)	11.9	0.289	0.738	0.301	0.233	0.742	0.085
acetonitrile (AN)	14.1	0.239	0.698	0.241	0.313	0.781	0.030
acetone (AC)	17.0	0.140	0.536	0.194	0.138	0.635	0.021
dimethylformamide (DMF)	26.6	−0.046	0.382	0.038	−0.024	0.632	0.007
dimethyl sulfoxide (DMSO)	29.8	−0.023	0.446	0.006	−0.010	0.697	0.014

[a] $E_{1/2}(1)$ and $E_{1/2}(2)$ are the first and second oxidation potentials observed in the 2:1 mixtures of the donor−acceptor; ref is fc/fc^+. The lower potential for each pair corresponds to the $(en)_2$ complex, the higher to the cyano complex. For techniques and conditions, see text.

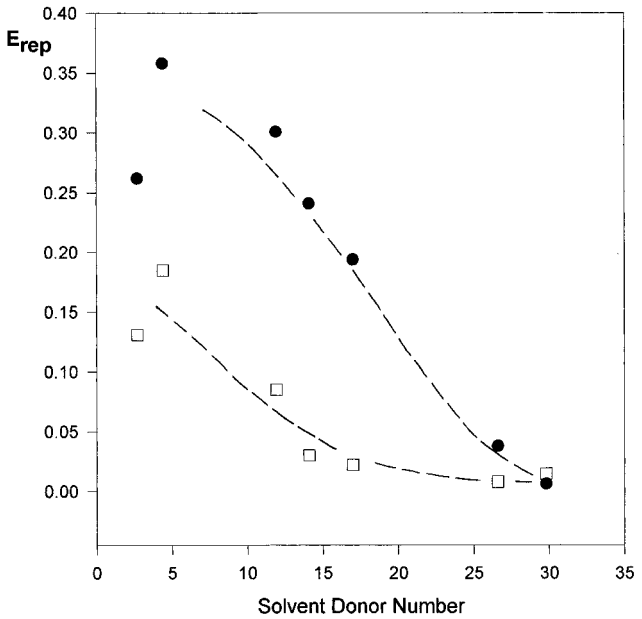

Figure 5. Variation of E_{rep} with solvent donor number for adducts **1** and **2**.

nitromethane we find $\Delta E_{1/2}' = 0.369$ V and $E_{rep} = 0.262$ V, and thus $\Delta G_{com} = 71.2$ kJ/mol with 50.6 kJ/mol due to the interaction.

The shifts in the redox potentials of the parent complexes upon adduct formation and hence the wave repulsion E_{rep} ultimately derive from some combination of electrostatic, solvational, statistical, and electronic delocalization effects.[6b,26b,27] We are unable to separate out the fraction of E_{rep} directly attributable to the electronic coupling between the sites. We can, however, use the spectroscopic information obtainable from the HBIT bands of the adducts (see Table 3) and eq 4 in order to arrive at an estimate for the electronic coupling matrix element, H_{ab}.[1c,6b,28,29]

$$H_{ab} = \{(2.05 \times 10^{-2})[\epsilon_{max}(\Delta\nu_{1/2})\nu_{max}]^{1/2}\}/d \qquad (4)$$

where ϵ_{max} is the extinction coefficient of the band, $\Delta\nu_{1/2}$ is the bandwidth, ν_{max} is the peak position, and d, in the simplest interpretation, is the geometric distance between the metal ions in angstroms.

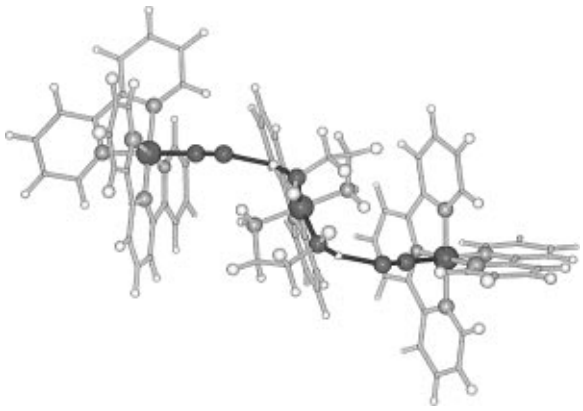

Figure 6. One of several possible structures arrived at by molecular mechanics calculations for adduct **1**. The H-bonding pathway is indicated with darkened bonds.

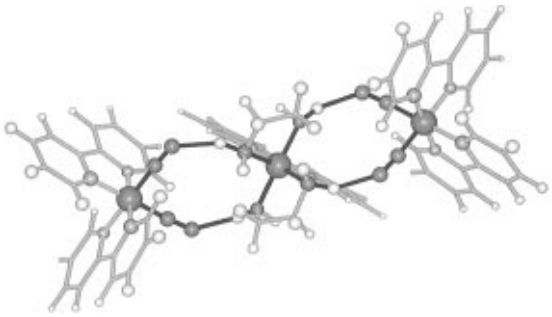

Figure 7. One of several possible structures arrived at by molecular mechanics calculations for adduct **2**. The H-bonding pathways are indicated with darkened bonds.

A key question concerns the number of H bonds assumed to be formed in each adduct. As discussed previously, the Job's plots of the low-energy HBIT bands maximize at a mole fraction of 0.65 (with respect to cyano complexes), thus indicating that the primary absorbing species is the 2:1 adduct. A number of reasonable structures for each of the adducts can be found to lie at similar energies by molecular mechanics calculations. Illustrations of possible structures for adducts **1** and **2** are shown in Figures 6 and 7. The simplest structural scenario involves a single, nonbifurcated hydrogen bond from an ethylenediamine nitrogen proton donor on the central Ru(III) to each cyano ligand on the terminal Ru(II) proton acceptor. Subtleties of the bonding in the adducts lead to a sizable range of plausible metal−metal

(27) (a) Sutton, J. E.; Sutton, P. M.; Taube, H. *Inorg. Chem.* **1979**, *18*, 1017. (b) Sutton, J. E.; Taube, H. *Inorg. Chem.* **1981**, *20*, 3125. (c) Richardson, D. E.; Taube, H. *Inorg. Chem.* **1981**, *20*, 1278.

(28) (a) Creutz, C. *Prog. Inorg. Chem.* **1983**, *30*, 1. (b) Newton, M. D.; Sutin, N. *Annu. Rev. Phys. Chem.* **1984**, *35*, 437. (c) Hush, N. S. *Coord. Chem. Rev.* **1985**, *64*, 135. (d) Sutin, N. *Adv. Chem. Ser.* **1991**, *228*, 25.

(29) Possible limitations of eq 4 in case of strongly-coupled systems have been discussed recently in the literature; see for example refs 26b and 30. The optical interaction in the systems studied here is fairly weak, however, and it is probable that the small-overlap limit appropriate to eq 4 is better-satisfied than in the systems discussed in refs 26b and 30.

(30) (a) Westmoreland, T. D.; Wilcox, D. E.; Baldwin, M. J.; Mims, W. B.; Solomon, E. I. *J. Am. Chem. Soc.* **1989**, *111*, 6106. (b) Mines, G. A.; Roberts, J. A.; Hupp, J. T. *Inorg. Chem.* **1992**, *31*, 125. (c) Dong, Y.; Hupp, J. T. *Inorg. Chem.* **1992**, *31*, 3170. (d) Endicott, J. F.; Xiaoqing, S.; Watzky, M. A.; Buranda, T.; Yabin, L. *Chem. Phys.* In press.

distances, as will be discussed below. We note that the assumption of single, nonbifurcated hydrogen bonds to each cyano ligand may seem drastic, but a review of the known structural data for relevant H bonds in metal ammine and cyano complexes generally supports this scenario.[31]

The values calculated for H_{ab} are obviously dependent upon the distance parameter used in eq 4. A survey of relevant structural data for H-bond lengths in transition metal cyano and ammine complexes indicates that the probable distance range for the H bonds between complexes such as the ones in this study is 2.1 ± 0.3 Å.[31] Using this range of H-bond distances in molecular mechanics calculations reveals various possible structures for the 2:1 adducts, depending on the ways in which the terminal Ru(II) end groups bond to either common or different ethylenediamine rings on the central Ru(III). We obtain H-bonded geometries with metal−metal distances ranging from 6.4 to 7.8 Å for monocyano adduct **1** and 5.7 to 6.6 Å for dicyano adduct **2**. These distance ranges in conjunction with the spectral data in Table 3 allow us to calculate average or representative H_{ab} values for the monocyano and dicyano groups of adducts. For the monocyano adducts at the mid-range metal−metal distance of 7.1 Å we obtain $H_{ab} = 0.028$ eV and a range of 0.031−0.025 eV if we consider our full estimated range for the probable metal−metal distance in the adduct. In the case of the dicyano group of adducts, we will make here the assumption implied in Figure 7 that equivalent H bonds are formed to each of the two cyano ligands on each of the two terminal cyano-bearing complexes, thus the interaction energies on a *per H-bond basis* are then one-half of those listed in Table 3. Within the confines of this assumption then, we arrive at a representative value of $H_{ab} = 0.034$ eV for the dicyano adducts at the midrange distance of 5.7 Å and a spread of $H_{ab} = 0.037-0.032$ eV over our estimated distance range.

Figure 8 allows us to compare the so-obtained H_{ab} estimates for the two groups of H-bonded adducts with data obtained from spectroscopic measurements on covalently bound mixed-valence dimeric systems. The upper dashed line (points **1**−**7**) is drawn from systems with conjugated nitrogen heterocyclic bridging ligands such as 4-cyanopyridine or 4,4′-bpy between ruthenium ammine termini. The next line down (open circles) is drawn through points calculated from the data reported by Stein and Lewis for a series of dithiaspiroalkane-bridged mixed-valence ruthenium ammine dimers.[32] The lower dashed line (closed circles) is drawn from the same data but with distances calculated on the basis of simple metal−metal distance through a "flattened" bridge (so as not to short-circuit the slight curvature of the bridge arrived at in some calculations) rather than the "through-bond" distance (which includes the tortuosity of the pathway) used by Stein and Lewis in their original analysis.[32,33]

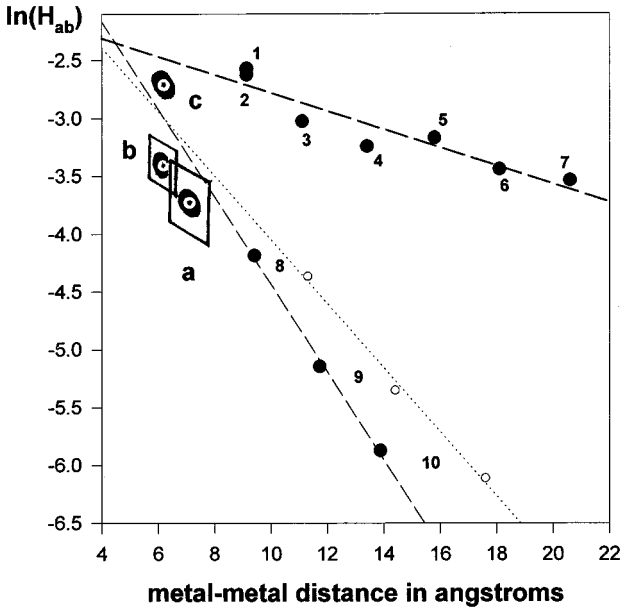

Figure 8. Ln(H_{ab}) *vs* metal−metal distance for (a) the monocyano-based adducts (from the data reported in Table 3) and (b) the dicyano-based adducts assuming two H bonds per metal−metal interaction (see text). Point c is for the dicyano adducts assuming only one H bond per metal−metal interaction. The upper line is for dimers with conjugated bridges: Dimer **1** is [(*trans*-py$(NH_3)_4$Ru$)_2$(4-cyanopyridine)]$^{5+}$ (from ref 26b), dimer **2** is [$((NH_3)_5$Ru$)_2$(4-cyanopyridine)]$^{5+}$ (from Richardson, D. E.; Taube, H. J. *Am. Chem. Soc.* **1983**, *105*, 40), dimer **3** is [$((NH_3)_5$Ru$)_2$(4,4′-bpy)]$^{5+}$ (from ref 27b), dimer **4** is [$((NH_3)_5$Ru$)_2$(bis-bipyridylethylene)]$^{5+}$ (from ref 27b); and dimers **5** through **7** are the dipyridylpolyene-bridged species (reported in ref 34). The lower lines are drawn from the data in ref 32 (as described in the text, see also ref 33) for the dithiaspiroalkane-bridged decaammine dimers. For dimer **8** there are two saturated rings in the bridge fused at a single spiro carbon, for dimer **9**, three rings, and for dimer **10**, four rings.

The large diamond-shaped regions represent the values obtained for the monocyano-based adducts (labeled **a** in the figure) and the dicyano-based adducts (labeled **b** in the figure). The sizes of these points are as large as they are due to the variablility of the H_{ab} values observed within each group of adducts (see Table 3) and the relatively large uncertainty in the metal−metal distance.

Nonetheless, it is clear that the electronic coupling in the H-bonded adducts is diminished relative to what would be expected for coupling through a σ-bonded covalent bridge at the same distance. Comparison with the H_{ab} values extrapolated from the dithiaspiroalkane-bridged systems indicates that the H bonds in both the mono- and the dicyano adducts are about 65−75% as efficient as σ-covalent bonds in establishing electronic coupling between the redox sites. Compared to π-conjugated bridging pathways (the upper dashed line), the coupling through the H bonds is about 30−40% as strong.

If the assumption of two H bonds to each dicyano complex in the dicyano-based adducts is dropped and simply the total metal−metal interaction energy plotted, then the point labeled **c** on the plot is obtained (full uncertainty region omitted for clarity). The position of this point turns out to be between the pure-σ and π-conjugated extrapolation lines, and it would imply a rather drastic changeover in coupling relative to the mono-cyano point a even though the estimated distances for both adducts are fairly similar. This does not seem likely, and we conclude that the dicyano complexes are probably doubly H bonded to the central unit—as assumed above. This idea is

(31) (a) Figgis, B. N.; Kucharski, E. S. *Acta Crystallogr.* **1991**, *B47*, 858−861. (b) Figgis, B. N.; Leung, P. C.; Schultz, A. J. *Acta Crystallogr.* **1985**, *C41*, 633−636. (c) Figgis, B. N.; Reynolds, P. A.; Williams, B. A.; Lehner, N. *Aust. J. Chem.* **1981**, *34*, 993−999. (d) Iwata, M.; Saito, Y. *Acta Crystallogr.* **1973**, *B29*, 822−832. (e) Iwata, M.; Saito, Y. *Acta Crystallogr.* **1977**, *B33*, 59−69. (f) Varetti, E. L.; Vergara, M. M.; Rigotti, B.; Navaza, A. *J. Phys. Chem. Solids* **1990**, *51*, 381−386. (g) Rigotti, B.; Aymonino, P. J.; Varetti, E. L. *J. Crystallogr. Spectrosc. Res.* **1984**, *14*, 517−530.

(32) (a) Stein, C. A.; Lewis, N. A.; Seitz, G. *J. Am. Chem. Soc.* **1982**, *104*, 2596−2599. (b) Stein, C. A.; Lewis, N. L.; Seitz, G.; Baker, A. D. *Inorg. Chem.* **1983**, *22*, 1124−1128. See also Rendell, A. P. L.; Bacskay, G. B.; Hush, N. S. *J. Am. Chem. Soc.* **1988**, *110*, 8343−8354.

(33) The metal−metal distances used in the lowest line of Figure 8 were arrived at via geometry optimization using the parametrization of ZINDO listed as ZINDO/1 in the Hyperchem 4.5 quantum chemistry software package (Hypercube). See: (a) Zerner, M. C.; Loew, G. H.; Kirchner, R. F.; Mueller-Westerhoff, U. T. *J. Am. Chem. Soc.* **1980**, *102*, 589.

(34) Woitellier, S.; Launay, J. P.; Spangler, C. W. *Inorg. Chem.* 1989, *28*, 758.

supported by the electrochemical wave repulsion data as well (*vide supra*). Here it was observed that the magnitude of the repulsion in low-donor media tended to be about twice as big for the dicyano-based adducts as for the monocyano ones (see Table 4 and Figure 5).

Concluding Remarks. The electrochemical and spectroscopic studies reported here prove that reasonably strong electronic coupling can occur through hydrogen bonds between inorganic complexes in solution. The formulations of the adducts are such that two cyano-based donors interact with one ethylenediamine-based acceptor, e.g., $[((bpy)_2Ru^{II}(CN)_2)_2,(en)_2Ru^{III}(bpy)]^{3+}$. Both the H_{ab} values, as evaluated from the spectra with the Hush equation,[1] and the magnitude of the electrochemical wave repulsion effect in low-donor solvents indicate that two H bonds to a given donor complex are approximately twice as effective as one in establishing the interaction. Analysis of the coupling energies relative to known covalently-bound dimeric species indicates that the magnitude of the coupling through the H bonds in these adducts is about 65−75% of what one would expect for a purely σ-bonded covalent pathway and about 30−40% of what would be expected for a π-conjugated pathway.

This result is in reasonable agreement with the estimate of near-equivalency for H-bonded segments and covalently-bonded ones as far as establishing tunneling pathways in proteins,[7] but it contrasts with the results of Therien and co-workers,[11] showing that in some cases H bonds can be even more effective at establishing electronic coupling. The difference may have to do with the fact that our current assessments are based on spectroscopic rather than thermal measurements, or it may simply be that the degree of electronic coupling through hydrogen bonds will turn out to be very case specific.

Acknowledgment. This work was made possible by the support of the National Science Foundation RUI program, Grant No. CHE-9200446. The ruthenium used was provided on loan from the Johnson-Matthey Aesar/Alpha Platinum Group Metals Loan Program. J.C.C. wishes to thank Prof. Stephan Isied of Rutgers University and Prof. N. S. Hush of the University of Sydney for valuable suggestions. We also wish to thank Prof. Henry Taube of Stanford for helpful discussions and for providing us with a preprint of ref 24.

JA962391G